Binocularly Asymmetric Crowding in Glaucoma and a Lack of Binocular Summation in Crowding

Foroogh Shamsi,[1] Rong Liu,[1–3] and MiYoung Kwon[1,2]

[1]Department of Psychology, Northeastern University, Boston, Massachusetts, United States
[2]Department of Ophthalmology and Visual Sciences, School of Medicine, University of Alabama at Birmingham, Birmingham, Alabama, United States
[3]Department of Life Science and Medicine, University of Science and Technology of China, Hefei, China

Correspondence: MiYoung Kwon, Department of Psychology, Northeastern University, 125 Nightingale Hall, 360 Huntington Ave., Boston, MA 02115, USA; m.kwon@northeastern.edu.

Received: August 26, 2021
Accepted: January 5, 2022
Published: January 27, 2022

Citation: Shamsi F, Liu R, Kwon M. Binocularly asymmetric crowding in glaucoma and a lack of binocular summation in crowding. *Invest Ophthalmol Vis Sci.* 2022;63(1):36. https://doi.org/10.1167/iovs.63.1.36

Purpose. Glaucoma is associated with progressive loss of retinal ganglion cells. Here we investigated the impact of glaucomatous damage on monocular and binocular crowding in parafoveal vision. We also examined the binocular summation of crowding to see if crowding is alleviated under binocular viewing.

Methods. The study design included 40 individuals with glaucoma and 24 age-similar normal cohorts. For each subject, the magnitude of crowding was determined by the extent of crowding zone. Crowding zone measurements were made binocularly in parafoveal vision (i.e., at 2° and 4° retinal eccentricities) visual field. For a subgroup of glaucoma subjects ($n = 17$), crowding zone was also measured monocularly for each eye.

Results. Our results showed that, compared with normal cohorts, individuals with glaucoma exhibited significantly larger crowding—enlargement of crowding zone (an increase by 21%; $P < 0.01$). Moreover, we also observed a lack of binocular summation (i.e., a binocular ratio of 1): binocular crowding was determined by the better eye. Hence, our results did not provide evidence supporting binocular summation of crowding in glaucomatous vision.

Conclusions. Our findings show that crowding is exacerbated in parafoveal vision in glaucoma and binocularly asymmetric glaucoma seems to induce binocularly asymmetric crowding. Furthermore, the lack of binocular summation for crowding observed in glaucomatous vision combined with the lack of binocular summation reported in a previous study on normal healthy vision support the view that crowding may start in the early stages of visual processing, at least before the process of binocular integration takes place.

Keywords: crowding, glaucoma, binocular summation, ganglion cell damage, crowding zone

Glaucoma is a leading cause of irreversible blindness worldwide, characterized by the progressive loss of retinal ganglion cells (RGCs) and the resultant visual field defects.[1] The conventional view has been that glaucoma spares central vision until the end stage and, thus, it has little impact on central visual function.[2–5] However, accumulating evidence has shown that even early glaucomatous injury involves the macula, and this macular damage is more common than generally thought.[6–13] For example, a number of anatomical studies[8,11,12,14–16] using spectral-domain optical coherence tomography have shown that the thickness of the retinal nerve fiber layer and the RGC plus inner plexiform layer (RGC+), even in the macula, are significantly thinner in patients with early glaucoma than in healthy controls. In parallel with anatomical evidence, perceptual evidence indicates noticeable deficits in assumed-to-be central vision tasks, such as reading and object/face recognition.[4,5,17–24] Given the conventional view, it is surprising that reading difficulty is a common complaint among patients with glaucoma.[3,23,25–31]

Although the exact perceptual mechanism limiting pattern recognition function in glaucoma remains unclear, converging evidence suggests that changes in visual crowding in glaucomatous vision may be one of the limiting factors.[32–36] Visual crowding refers to the inability to recognize a target object in clutter[37] on account of the deleterious influence of nearby items on visual recognition.[38] In real life, objects rarely appear in isolation. Therefore, the ability to isolate the target item from nearby clutter plays a critical role in everyday visual function such as reading, face recognition, and visual search.[39–43] Because the observers have no difficulty recognizing objects in the same retinal eccentricity in the absence of clutter, the phenomenon of crowding cannot be simply accounted for by decreased visual acuity or a loss of contrast sensitivity. Although the exact locus and mechanism of crowding remain under debate, a

Copyright 2022 The Authors

This work is licensed under a Creative Commons Attribution-NonCommercial-NoDerivatives 4.0 International License.

Downloaded from intl.iovs.org on 08/15/2022

Investigative Ophthalmology & Visual Science

popular explanation is that features of the target and flankers are integrated inappropriately due to a large integration zone (or perceptive pooling region), which results in relevant features being perceptually indistinguishable.[44–51] Crowding grows with increasing retinal eccentricity as the receptive (perceptive) field size increases in the periphery (i.e., scale shift).[37,52,53] Although very little crowding exists in normal central/parafoveal vision,[54] some clinical conditions like amblyopia manifest noticeably increased foveal crowding, which correlates with reading rate.[39,55,56] Hence, crowding, particularly in the central visual field, can be a good indicator of a person's everyday visual function.

Thus, the current study was undertaken to examine whether crowding is indeed exacerbated in parafoveal vision of glaucomatous eyes (i.e., the central 8° visual field), the visual field relevant to daily visual function. The relationship between crowding and glaucomatous damage was investigated in two ways: a between-subjects study design comparing crowding between patients with glaucoma and age-similar normal controls and a within-subjects study design comparing crowding between the worse eyes and the better eyes of patients with glaucoma. We, thus, hypothesized that the parafoveal crowding would be significantly larger in the glaucomatous vision compared with the age-matched normal vision and in the worse eye compared with the better eye.

Furthermore, because glaucoma is often bilateral and asymmetry is common, this binocularly asymmetry in glaucomatous damage provides us with a unique opportunity to explore the binocular summation of crowding. Binocular summation refers to an increase in binocular performance over monocular performance that is often quantified as a ratio of visual performance or sensitivity of the binocular to that of the better eye.[57–59] Previous studies on contrast sensitivity or visual acuity have reported binocular summation ratio of 1.4 (i.e., a 40% increase in binocular condition) or beyond in normal vision.[58,60–62]

However, little is known about how the crowding effect is integrated between two eyes. Thus, the secondary aim of the current study was to explore the mechanism of binocular summation in crowding.

To this end, we assessed binocular crowding in both patients with glaucoma (n = 40) and in age-similar normal controls (n = 24). Crowding was assessed with a well-established method: the spatial extent of crowding (i.e., threshold spacing between the target and flankers required to yield a criterion recognition accuracy). Crowding measurements were made in parafoveal vision (i.e., retinal eccentricity of 2° or 4°). For the binocular summation analysis, both monocular and binocular crowding were measured in a subset of patients with glaucoma.

Methods

Participants

A total of 68 subjects participated in the current study: 44 patients with bilateral primary open-angle glaucoma (mean age, 63.66 ± 8.91 years) and 24 age-similar normal control subjects (mean age, 60.21 ± 9.56 years). Patients with bilateral glaucoma and control subjects were recruited from the Callahan Eye Hospital Clinics at the University of Alabama at Birmingham. Patients with glaucoma whose diagnosis was confirmed through medical records met the following inclusion criteria in both eyes: (i) glaucoma-specific changes of the optic nerve or a nerve fiber layer defect. The presence of the glaucomatous optic nerve was defined by masked review of optic nerve head photos by glaucoma specialists using previously published criteria.[60] (ii) Glaucoma-specific visual field defect: a value of Glaucoma Hemifield Test from the Humphrey Field Analyzer (HFA) must be outside normal limits. (iii) No history of other ocular or neurological disease or surgery that caused visual field loss.

Visual field tests were performed with standard automatic perimetry using SITA Standard 24–2 and 10-2 tests with an HFA (Carl Zeiss Meditec, Inc., Jena, Germany). Goldmann size III targets with a diameter of 0.43° were presented for 200 ms at one of 54 (68) test locations for 24-2 (10-2) in a grid on a white background (10 cd/m^2).

The average mean deviation obtained from the HFA (24-2 test) in patients with glaucoma was −8.55 ± 9.75 dB for the right eye and −10.93 ± 8.43 dB for the left eye. According to the Hodapp–Anderson–Parrish glaucoma grading system,[63] the majority of our patients with glaucoma were either in the early or moderate stages of glaucoma. The mean binocular visual acuity (Early Treatment Diabetic Retinopathy charts) for patients with glaucoma was −0.01 ± 0.10 logMAR (or 20/20 Snellen equivalent). The mean monocular visual acuity was 0.09 ± 0.18 logMAR for the right eye and 0.10 ± 0.16 logMAR for the left eye. The mean binocular log contrast sensitivity (Pelli–Robson charts) was 1.69 ± 0.19.

Normal vision was defined as better than or equal to 0.2 logMAR best-corrected visual acuity in each eye with normal binocular vision (confirmed through preliminary vision tests including the Worth four dot test, Stereo Fly vision test, HFA, visual acuity, and contrast sensitivity) and with no history of ocular or neurological disease other than cataract surgery. The mean binocular visual acuity for normal control subjects was −0.07 ± 0.08 logMAR (or 20/20 Snellen equivalent). The mean monocular visual acuity was −0.01 ± 0.08 logMAR for the right eye and −0.01 ± 0.1 logMAR for the left eye. The mean binocular log contrast sensitivity for normal controls was 1.92 ± 0.10.

All participants were native or fluent English speakers without known cognitive or neurological impairments, confirmed by the Mini Mental Status Exam (score of ≥25). The main experiments were conducted with binocular viewing (n = 40). This was done to assess the amount of crowding relevant to real-life visual tasks. Proper refractive correction for the viewing distance was used. For a subset of patients with glaucoma (n = 17), the experiments were also performed under a monocular viewing condition. The number of subjects with both binocular and monocular crowding measurements was 13. For the subjects with both binocular and monocular measurements, the binocular and monocular experiments were performed on different days and monocular measurements were done after the binocular measurement. The experimental protocols followed the tenets of the Declaration of Helsinki and were approved by the Internal Review Board at the University of Alabama at Birmingham. Written informed consents were obtained from all participants before the experiment after explanation of the nature of the study.

Stimulus and Apparatus

For the crowding task, the stimuli consisted of a target letter flanked by four tumbling Es on four cardinal sides of the target. The target letter was randomly drawn from a set of

Investigative Ophthalmology & Visual Science

Downloaded from intl.iovs.org on 08/15/2022

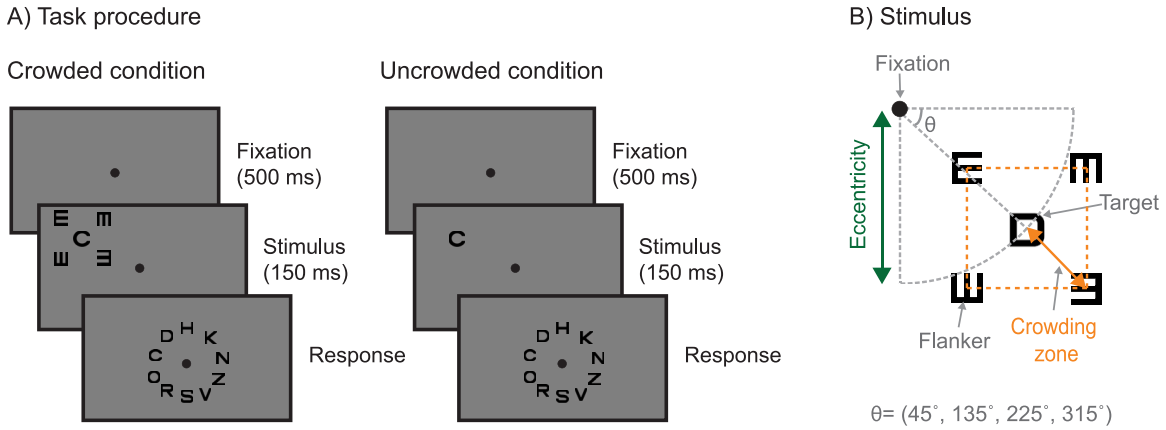

Figure 1. Measuring crowding zone. (**A**) Task procedure for crowded and uncrowded conditions. A target letter with/without flankers was presented at the assigned location for 150 ms, which was followed by a response interval. During the response interval, participants were asked to choose the target letter they saw during the stimulus interval using a subsequent letter panel. (**B**) Stimulus for crowded condition. An illustration of the stimulus configuration for measuring the spatial extent of crowding (i.e., crowding zone). A target letter ("D" in this example) was located at one of two distances from the fixation (2° or 4°), and at one of four azimuth angles around the fixation (Θ = 45°, 135°, 225°, or 315°). Four flankers ('E' rotated at four different orientations) were located at four orthogonal locations with the same distance from the target. Crowding zone represents the distance between target and flankers required to yield 79.4% letter-recognition accuracy. The larger crowding zone, the larger detrimental effect from nearby clutter.

10 Sloan letters: CDHKNORSVZ. All the letters were black on a uniform gray background (159 cd/m^2) with a contrast of 99%, and a letter size of 0.8° (x-height). The fixation dot used in this experiment was a black circle in the center of the screen spanning 0.25° of the visual field. All stimuli were generated and controlled using MATLAB (version 8.3) and Psychophysics Toolbox extensions (version 3)[64,65] for Windows 7, running on a PC desktop computer (model: Dell Precision Tower 5810). Stimuli were presented on a liquid crystal display monitor (model: Asus VG278HE; refresh rate: 144 Hz; resolution: 1920 × 1080, graphic card: 2 GB Nvidia Quadro K2000, subtending 60° × 34° visual angle at a viewing distance of 57 cm) with the mean luminance of the monitor at 159 cd/m^2. The luminance of the display monitor was made linear using an 8-bit look-up table in conjunction with photometric readings from a MINOLTA LS-110 Luminance Meter (Konica Minolta Inc., Tokyo, Japan).

Measuring the Spatial Extent of Crowding (Crowding Zone)

The crowding effect was measured by determining the spatial extent of crowding. Threshold spacing (or crowding zone) was defined as the center-to-center distance between the high-contrast target and flankers that yields a target-identification accuracy of 79.4%. Thus, threshold spacing becomes larger with increasing crowding. A subject's threshold spacing was estimated at eight retinal locations: two retinal eccentricities (2° or 4°) and four azimuth angles around the fixation (45°, 135°, 225°, or 315°) (Fig. 1), using a three-down-one-up staircase procedure[66] with a step size of 15%. The total number of staircase reversals were set to nine and the threshold spacing was determined by taking the geometric average of the last seven staircase reversals. For each retinal location, a target letter was flanked by four tumbling Es. At each block, one of the eight target locations was tested. The tested location was predetermined for each block and counterbalanced across blocks to minimize the order effect. At the beginning of each block, to cue participants, a small red dot was shown at the target location. Then, the subject pressed a key on the keyboard to initiate the experiment block. In each trial, a target letter with flankers was presented at the assigned location for 150 ms (approximately 22 frames = 152.7 ms). During the last trial of each block, the target letter was presented at the same location without flankers (i.e., uncrowded condition). Participants were instructed to fixate on a central dot during the stimulus presentation and to report the target letter they saw during the stimulus interval in a subsequent response interval (as shown in Fig. 1A) by clicking the mouse on the selected letter. No time limit was considered for the subjects' responses and they responded at their own pace. Auditory feedback was given whenever the correct answer was chosen. The spacing between the letters in the response panel was fixed and the letters in the response panel were uniformly spaced in a circle with the radius of 5° eccentricity. It should be noted that the subjects did not have to maintain their central fixation during the response interval. The time interval between the offset of the stimulus and the onset of the response panel was set to 500 ms. The task procedure was the same for monocular and binocular measurements.

A chinrest was used to minimize head movements. The experimenter visually observed subjects to confirm that fixation instructions were followed. Note that the stimulus duration (150 ms) was too short to allow for any reliable saccadic eye movements (considering the fact that the average saccades usually take about 230 ms and up to 250 ms). Therefore, the subjects knew there was no advantages in moving their eye during the stimulus duration. All subjects had practice trials for both crowding and visual span tasks before data collection. A subject's stable fixation was also monitored using a high-speed eye tracker (EyeLink 1000 Plus/Desktop mount, SR Research Ltd., Kanata, Ontario, Canada).

Downloaded from intl.iovs.org on 08/15/2022

Data Analysis

The normality of the data was checked using the quantile–quantile plot. To examine if there are any significant differences in crowding effect between (i) retinal eccentricities and (ii) patients with glaucoma and age-matched normal cohorts, we performed an ANOVA on crowding zone – 2 (retinal eccentricity: 2° and 4°) × 2 (subject group: glaucoma and normal cohorts) repeated measures ANOVA with retinal eccentricity as a within-subject factor. To determine which specific groups differ from each other, we also performed Tukey's HSD post hoc test. Statistical analyses were performed using MATLAB software (version (R2020b; The MathWorks Inc., Natick, MA).[67] The ratio between the crowding zone of the individual glaucoma subjects with respect to the average crowding of the age-matched normal control group as well as the ratio of the average of the two groups were calculated at two eccentricities (2° and 4°). To compare the binocular with monocular crowding, we categorized the data into worse and better eyes based on the crowding values (i.e., more and less crowded eyes) and calculated the average crowding for the better and worse eyes and compared them with the average binocular crowding. The binocular summation ratio of crowding is defined as the ratio of binocular crowding to the crowding of the better eye. To follow the notion that the summation ratio of more than 1 indicates the binocular summation, we used the inverse value of crowding for calculating the binocular summation ratio, that is, the binocular summation ratio $= \frac{1/\text{binocular crowding}}{1/\text{better eye crowding}}$.

Results

Increased Binocular Crowding in the Parafoveal Vision of Patients With Glaucoma

We first compared binocular crowding between glaucoma and normal controls to see if glaucomatous damage indeed increases the binocular crowding in parafoveal vision (i.e., the retinal eccentricity of 2° and 4°). Figure 2A plots the extent of binocular crowding zone (i.e., a threshold spacing between the target and flankers required to recognize the target with 79.4% accuracy) at each testing location in polar coordinates. The binocular crowding zone data from 10 exemplary individuals with glaucoma (orange lines) were compared with the average crowding of normal control subjects at different testing locations (green lines). A greater extent of crowding zone indicates increased crowding. It is apparent that the crowding zone of the patient with glaucoma is noticeably larger than that of the normal control subject at each testing location. As expected, we also observed increasing crowding zone with increasing eccentricity.

The same pattern of the results is summarized in the group average data. The left panel in Figure 2B plots the extent of binocular crowding zone as a function of retinal eccentricity (2° and 4°) for patients with glaucoma (orange dots) and normal cohorts (green dots). Each dot represents the data point from an individual subject. The crowding zone results were averaged across the four different testing locations (Θ = 45°, 135°, 225°, or 315°) as no significant differences were found across testing locations with the same eccentricity (2° or 4°) for both glaucoma, $F_{(3, 156)} = 1.3$, $P = 0.28$ for 2° and $F_{(3, 156)} = 2.27$, $P = 0.08$ for 4°, and normal groups, $F_{(3, 156)} = 0.76$, $P = 0.52$ for 2° and $F_{(3, 156)} = 0.92$, $P = 0.43$ for 4°. A two-way repeated measures ANOVA showed a significant main effect of subject group, $F_{(1, 62)} = 9.49$, $P = 0.003$, on crowding zone. There was also a significant interaction effect between subject group and eccentricity, $F_{(1, 62)} = 6.00$, $P = 0.017$. A pairwise comparison test further showed that the crowding zone of the glaucoma group is significantly larger than that of the normal control group for all test eccentricities ($P = 0.001$ and 0.005 for 2° and 4° eccentricities, respectively). As shown in the right panel of Figure 2B, on average the crowding zones of the glaucoma group are 13% and 27% larger than those of the normal controls for 2° and 4° eccentricities, respectively. There was also a significant main effect of eccentricity on crowding zone, $F_{(1.62)} = 102.94$, $P < 0.001$. Consistent with earlier findings,[37,53] pairwise comparison test showed that the crowding zone becomes increasingly larger with increasing eccentricity for both glaucoma and normal controls (all Ps < 0.001).

It is also noteworthy that the recognition accuracy results for the uncrowded condition averaged across two eccentricities (2° and 4°) were 95% and 98% for glaucoma and normal groups, respectively (Fig. 2C).

Increased Monocular Crowding in the Eyes With More Severe Glaucoma

To further confirm the effects of the glaucoma on crowding, we capitalized on the fact that the severity of glaucomatous damage tends to differ between the two eyes. Monocular crowding zone were measured monocularly at 2° and 4° eccentricities for a group of glaucoma subjects (n = 17) using the same experimental paradigm as the binocular crowding zone measurement. Crowding zone of the worse eye (i.e., the eye with more severe glaucomatous damage) was compared with that of the better eye. The worse and better eyes were determined based on the mean deviation value from the HFA 10-2 test (i.e., perimetry in the central 10° visual field), where more negative mean deviation is considered to be more severe glaucoma.

Figure 3A (i) plots the extent of the monocular crowding zone at each testing location in polar coordinates for the worse (solid line) and better (dotted line) eyes of an exemplary glaucoma subject. The results of comparing the average crowding zone of the worse and better eyes for all subjects are summarized in Figure 3A (ii). Gray circles indicate the average monocular crowding zone across different testing locations for the worse and better eyes. The extent of monocular crowding zone was compared between the worse eye (orange solid bounding boxes) and better eye (orange dotted bounding boxes) for 2°, 4°, and both eccentricities. To visualize the binocular asymmetry in crowding present in an individual subject, measurements between the two eyes of a single subject are connected by a gray solid line. We observed significantly larger crowding in the worse eyes compared with the better eyes, $t_{(32)} = 2.34$, $P < 0.05$.

No Evidence of Binocular Summation or Inhibition in Crowding

In the foregoing session, we showed that the binocularly asymmetric glaucomatous damage brings about corresponding binocularly asymmetric crowding. This asymmetry in the monocular crowding provided us with a unique opportunity to explore the binocular combination of crowding.

Investigative Ophthalmology & Visual Science

Downloaded from intl.iovs.org on 08/15/2022

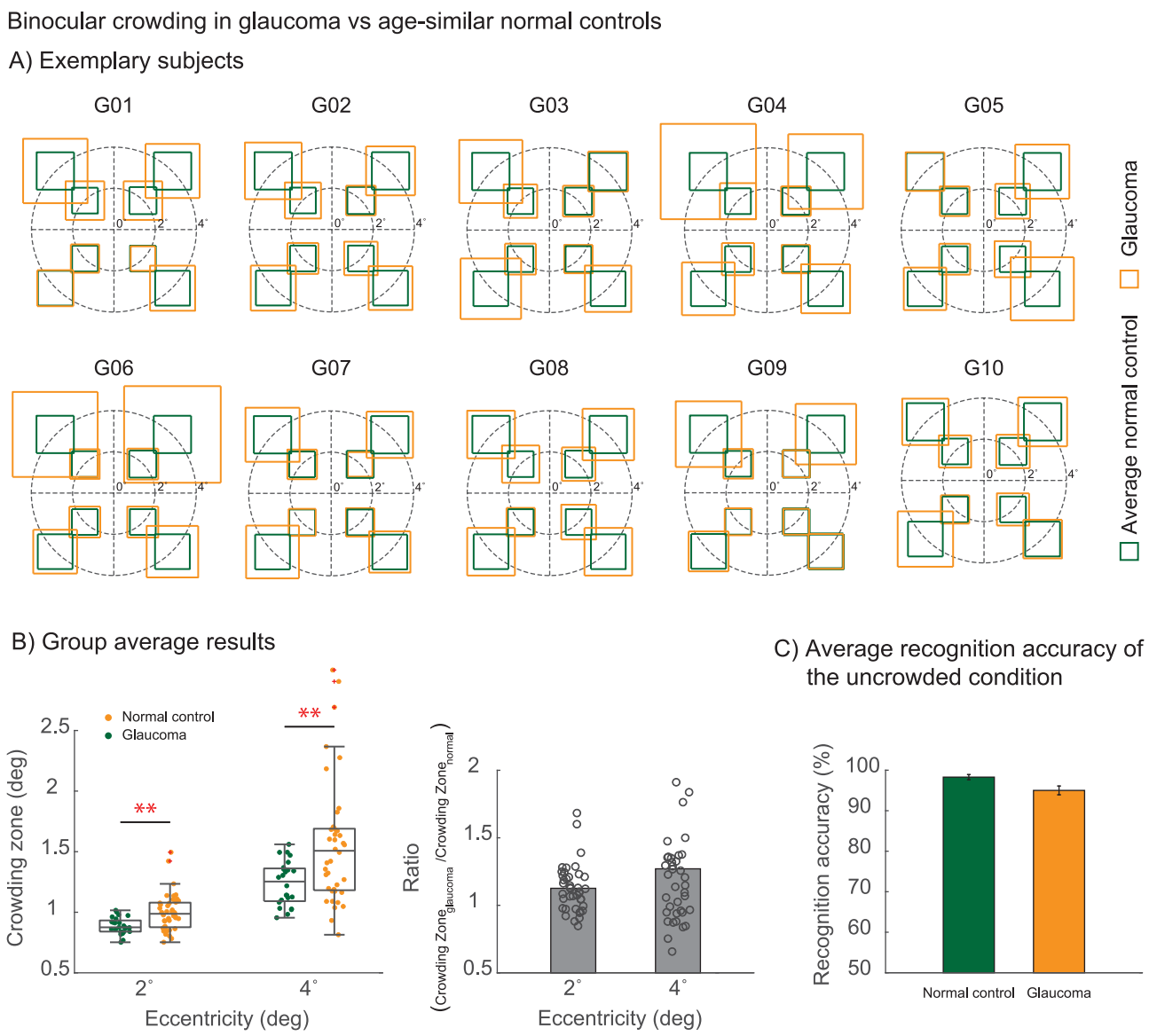

Figure 2. Binocular crowding in glaucoma vs age-similar normal controls. (**A**) Exemplary subjects. The extent of crowding zone at each testing location was plotted in polar coordinates for 10 individuals with glaucoma (*orange*) and the average of normal subjects (*green*). (**B**) Group average results. (*Left*) The crowding zone averaged across testing locations (Θ = 45°, 135°, 225°, or 315°) are plotted as a function of eccentricity (2° and 4°): patients with glaucoma (*orange dots*) and normal cohorts (*green dots*). Each dot represents the data point from an individual subject. (*Right*) Mean ratio of the crowding zone of patients with glaucoma to that of normal cohorts (ratio = crowding $\text{zone}_{\text{glaucoma}}$/crowding $\text{zone}_{\text{normal control}}$) was plotted as a function of eccentricity. Individual data points are the ratio of the crowding for individual patients with glaucoma to the mean crowding of the normal group at two eccentricities. Note that ** indicates statistical significance at a P value of less than 0.01. (**C**) Average recognition accuracy of uncrowded condition. Bar graphs represent the average recognition accuracy of uncrowded condition for glaucoma (*orange*) and normal control (*green*) groups.

Binocular summation often refers to an increase in the binocular performance over the monocular performance. We, thus, examined a potential binocular advantage in crowding. To this end, we obtained both monocular and binocular crowding measurements in a subset of patients with glaucoma (n = 13). Binocular summation was quantified as the ratio of crowding of the binocular to that of the better eye (i.e., the eye with less crowding). A ratio value of greater than 1 would indicate binocular summation, whereas a value of equal to or less than 1 would indicate no binocular summation or inhibition. Note that, to follow the notion that the binocular summation ratio of greater than 1 indicates binocular summation, we considered the inverse values for calculating the summation ratio, that is, 1/crowding. Figure 3B (i) shows the average of monocular crowding zone for the worse and better eyes as well as the binocular crowding zone. It should be noted that, here, the worse and better eyes are considered as the eyes with larger and smaller monocular crowding zones, respectively. Figure 3B (ii) plots the mean and individual data of the binocular ratio for crowding. As shown in Figure 3B (ii), the mean binocular ratio for crowding is 1, $t_{(12)} = -0.015$, $P = 0.99$, suggesting that the binocular

Investigative Ophthalmology & Visual Science

Downloaded from intl.iovs.org on 08/15/2022

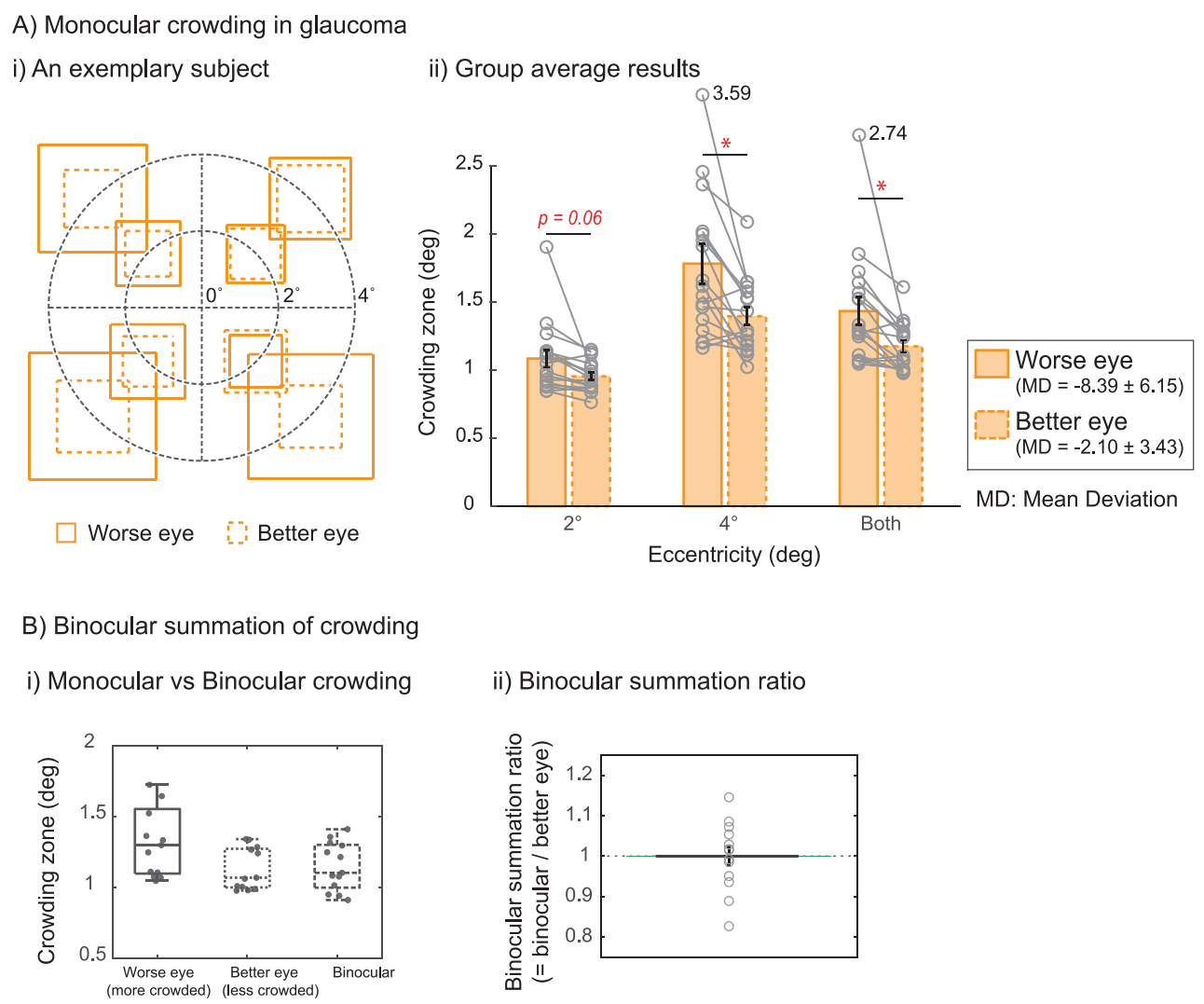

Figure 3. (**A**) Monocular crowding in glaucoma. (**i**) An exemplary subject. The extent of monocular crowding zone at each testing location is plotted in polar coordinates for the worse (*solid line*) and better (*dashed line*) eyes. (**ii**) Group average results. The extent of monocular crowding zone is compared between the worse eye (orange solid bounding boxes) and better eye (orange dotted bounding boxes) for 2°, 4°, and both eccentricities. Measurements between the two eyes of a single subject are connected by a gray solid line. Note that the worse and better eyes were determined for each subject based on the mean deviation (MD) values from HFA 10-2 test. Note that * denotes statistical significance at a *P* value of less than 0.05. (**B**) Binocular summation of crowding. (**i**) Monocular versus binocular crowding. The boxplots represent the extent of monocular crowding zone for the worse and better eyes and binocular crowding zone. Note that here, the worse and better eyes refer to eyes with larger (more crowded) and smaller (less crowded) crowding zones, respectively. Each gray dot represents the data point from an individual subject. (**ii**) Binocular summation ratio. Binocular summation ratio defined as the crowding of the binocular to that of the better eye. Note that we used the inverse values of crowding for calculating the binocular summation ratio to follow the notion that the binocular summation ratio of greater than 1 indicates the binocular summation.

crowding follows the better eye's performance without any binocular summation or inhibition.

Discussion

In this study, we showed that glaucomatous damage is associated with increased crowding even in the parafoveal region corresponding with the central 8° visual field (−4° to +4°). We found a statistically significant increase in the binocular crowding in patients with glaucoma relative to age-similar normal controls.

More important, to control for the possible effect of relatively higher cognitive factors such as attention or memory lapse between the stimulus interval and the response interval and low-level sensory factors such as acuity limit or decreased contrast for a peripheral target location on the behavioral results, our study design included the uncrowded experiment as a control condition (Fig. 1A). The results showed that both patients with glaucoma and normal controls were able to recognize a "single letter" (i.e., a target without flankers) at a given retinal eccentricity with a high level of accuracy (95% and 98% for glaucoma and normal groups, respectively). This result further assured us that our subjects had no trouble recognizing the target letter at a given retinal location when presented alone. Therefore, the observed difference in crowding between glaucoma and normal cohorts is likely to be due to the crowding effect rather than decreased acuity or contrast sensitivity at a given

Investigative Ophthalmology & Visual Science

Downloaded from intl.iovs.org on 08/15/2022

target location or other high-level cognitive factors, such as a lack of attention or memory lapse. The binocular visual acuity of these patients with glaucoma (−0.01 vs. −0.07 logMAR) and log contrast sensitivity (1.70 vs. 1.92) were comparable with those of normal controls, further supporting the view that signal letter acuity or contrast sensitivity were not likely plausible explanations for our findings. It should also be noted that the time interval between the offset of the stimulus and the onset of the response panel was set to 500 ms, which is much longer than the duration that likely induces backward masking (<50 ms). We, however, cannot completely rule out the possible role of backward masking on our results. Even if backward masking had played a role, it should have affected both the glaucoma and the age-matched normal cohorts equally.

It should be noted that we compared the crowding effect between glaucomatous and normal vision under binocular viewing, because binocular visual recognition likely reflects what patients would experience in real life. However, to further investigate the linkage between the severity of glaucomatous damage on crowding, we went on to measure the monocular crowding in patients with glaucoma using within-subjects comparison. Comparing the monocular crowding between the worse and better eyes defined by the severity of glaucoma-induced damage (i.e., mean deviation values) indeed confirmed larger crowding with more severe glaucomatous damage. This, in turn, can lead to asymmetrical monocular crowding in glaucomatous vision. Here we used this opportunity to address the question of how the binocular asymmetry in glaucomatous damage can affect the way crowding effect is integrated between two eyes (i.e., summation or inhibition).

Our findings showed that the glaucomatous vision did not exhibit binocular summation of crowding as the binocular crowding was determined by the better eye. This absence of binocular summation is consistent with a previous study done by Siman-Tov et al.[68]

They examined target recognition performance (in dprime) with or without distractors under both monocular and binocular viewing conditions. They found that the binocular summation was nearly absent when the target appeared in clutter for a stimulus duration of less than 240 ms. In contrast, the single target condition yielded binocular summation of about 1.4 (an 40% increase), as expected from previous findings.[58,60–62] Taken together, this absence of binocular summation for crowding suggests that crowding is likely to start at least before the process of binocular combination or integration known to take place or occur in the primary visual cortex (V1).[69,70] It is, however, worth mentioning that a bigger sample size may be required to confirm these results in a future study.

In normally sighted subjects, crowding has minimal impact on daily central vision tasks, because very little crowding exists in foveal or parafoveal regions.[38] However, people with some clinical conditions such as amblyopia are known to experience considerable crowding, even in their foveal vision; their functional deficits in central vision tasks such as reading and word recognition have been shown to correlate with the increased foveal crowding.[39,55,71–73] Because feature segmentation and integration are the core processes of visual recognition, crowding—the inability to isolate the target item from nearby distractors—is an essential bottleneck for visual recognition.[38] Therefore, determining whether individuals with impaired vision experience increased crowding is an important step toward a better understanding of daily pattern vision in clinical populations.

Glaucoma is typically thought to be peripheral vision loss, with central vision being preserved by the damage until the end stage of the disease. For this reason, little attention has been paid to understanding central pattern recognition function in glaucoma. However, recent research[8,11,12,14,15,74] using optical coherence tomography or retinal staining techniques has demonstrated significant structural damage even in early glaucoma. Such damage includes loss of RGCs or significant shrinkage of dendritic structure and cell body of remaining cells in the macula.

Various models have been put forward to explain the phenomenon of crowding. These models include, but are not limited to, low-level feature integration,[54,75,76] mid-level visual processing such as grouping,[77,78] substitution,[79] summary statistics,[46–49] saccade-confounded image statistics,[80] and higher level attentional account.[50] Although crowding is known to be a cortical phenomenon, the question regarding the exact mechanism and locus of the crowding remains a subject of debate. Despite various accounts of crowding, there is one common thread: crowding is ascribed to signals being pooled over a greater spatial extent (extensive pooling)[81] either owing to bottom-up computations,[35,45] such as hardwired integration fields, and/or top-down cognitive factors,[50] such as a spotlight of attention.

Thus, it is reasonable to speculate that glaucomatous damage, such as loss of ganglion cells, may bring about changes in the way visual signals are integrated across space, thereby leading to changes in crowding. Numerous studies have shown alterations in spatial summation mechanisms after glaucomatous damage. Redmond et al.[82] reported significant enlargement of Ricco's area in early glaucoma with respect to healthy subjects. A similar increase in the extent of Ricco's area was also observed by Mulholland et al.[83] Ricco's area is regarded as the spatial extent over which visual signals are integrated for the system to achieve threshold detectability and has been linked to ganglion cell density. It has been proposed that, to maintain threshold detectability in the presence of glaucomatous ganglion cell loss, the system actively compensates the loss by integrating signals over a larger area.[84,85] This view is also consistent with the inverse relationship between threshold stimulus size and RGC density reported in a number of psychophysical studies.[85–87] A close linkage between the sampling density of RGCs and the extent of spatial integration such as Ricco's area or crowding zone has also been demonstrated by the work done by our group.[35] Furthermore, King et al.[88] provided the neural basis of changes in summation mechanisms following glaucomatous damage. They found that the size of receptive field sizes in the adult rat brain increases in response to experimentally induced ganglion cell death. The increase of receptive fields was proportional to the degree of glaucomatous damage, highlighting the close linkage between the size of signal integration zones and ganglion cell damage. It is also important to note that the macular RGC+ layer thickness is closely correlated with RGC counts[89–91]: the thinner the layer gets, the more the RGCs are being lost.

We, however, acknowledge that a more quantitative relationship between the degree of crowding and severity of glaucomatous damage needs to be explored in future studies. Perhaps, a cross-sectional study with different stages of the disease progression, including preperimetic glaucoma,

Investigative Ophthalmology & Visual Science

Downloaded from intl.iovs.org on 08/15/2022

will help us to further characterize the relationship between the two.

In summary, the current study shows that crowding is exacerbated in parafoveal vision in glaucoma and binocularly asymmetric glaucoma is associated with binocularly asymmetric crowding. Our findings are consistent with the view that glaucomatous damage brings about alterations in spatial pooling mechanisms. Furthermore, the absence of binocular summation for crowding observed in glaucomatous vision combined with the lack of binocular summation found in Siman-Tov et al.'s[68] normal healthy vision support the view that crowding may start in the early stages of visual processing, at least before the process of binocular integration takes place.

Acknowledgments

Supported by NIH/NEI Grant R01 EY027857, Research to Prevent Blindness (RPB) / Lions' Clubs International Foundation (LCIF) Low Vision Research Award, and Eyesight Foundation of Alabama.

Disclosure: **F. Shamsi,** None; **R. Liu,** None; **M. Kwon,** None

References

1. Friedman DS, Wolfs RC, O'Colmain BJ, et al. Prevalence of open-angle glaucoma among adults in the United States. *Arch Ophthalmol*. 2004;122:532–538, doi:10.1001/archopht.122.4.532.
2. Ramulu P. Glaucoma and disability: which tasks are affected, and at what stage of disease? *Curr Opin Ophthalmol*. 2009;20:92–98, doi:10.1097/ICU.0b013e32832401a9.
3. Stamper RL. The effect of glaucoma on central visual function. *Trans Am Ophthalmol Soc*. 1984;82:792–826.
4. Stamper RL. Psychophysical changes in glaucoma. *Surv Ophthalmol*. 1989;33(Suppl):309–318.
5. Burton R, Crabb DP, Smith ND, Glen FC, Garway-Heath DF. Glaucoma and reading: exploring the effects of contrast lowering of text. *Optom Vis Sci*. 2012;89:1282–1287, doi:10.1097/OPX.0b013e3182686165.
6. Quigley HA, Addicks EM, Green WR. Optic nerve damage in human glaucoma: III. Quantitative correlation of nerve fiber loss and visual field defect in glaucoma, ischemic optic neuropathy, papilledema, and toxic optic neuropathy. *Arch Ophthalmol*. 1982;100:135–146.
7. Elze T, Pasquale LR, Shen LQ, Chen TC, Wiggs JL, Bex PJ. Patterns of functional vision loss in glaucoma determined with archetypal analysis. *J R Soc Interface*. 2015;12:0141118, doi:10.1098/rsif.2014.1118.
8. Hood DC, Raza AS, de Moraes CG, Liebmann JM, Ritch R. Glaucomatous damage of the macula. *Prog Retin Eye Res*. 2013;32:1–21, doi:10.1016/j.preteyeres.2012.08.003.
9. Medeiros FA, et al. Retinal ganglion cell count estimates associated with early development of visual field defects in glaucoma. *Ophthalmology*. 2013;120:736–744, doi:10.1016/j.ophtha.2012.09.039.
10. Anctil J-LA, Douglas R. Early foveal involvement and generalized depression of the visual field in glaucoma. *Arch Ophthalmol*. 1984;102:363–370.
11. Hood DC, Raza AS, de Moraes CG, et al. Initial arcuate defects within the central 10 degrees in glaucoma. *Invest Ophthalmol Vis Sci*. 2011;52:940–946, doi:10.1167/iovs.10-5803.
12. Hood DC, Raza AS, de Moraes CG, Johnson CA, Liebmann JM, Ritch R. The nature of macular damage in glaucoma as revealed by averaging optical coherence tomography data. *Transl Vis Sci Technol*. 2012;1:3, doi:10.1167/tvst.1.1.3.
13. Chen S, McKendrick AM, Turpin A. Choosing two points to add to the 24-2 pattern to better describe macular visual field damage due to glaucoma. *Br J Ophthalmol*. 2015;99:1236–1239, doi:10.1136/bjophthalmol-2014-306431.
14. Hood DC, Slobodnick A, Raza AS, de Moraes CG, Teng CC, Ritch R. Early glaucoma involves both deep local, and shallow widespread, retinal nerve fiber damage of the macular region. *Invest Ophthalmol Vis Sci*. 2014;55:632–649, doi:10.1167/iovs.13-13130.
15. Wang M, Hood DC, Cho JS, et al. Measurement of local retinal ganglion cell layer thickness in patients with glaucoma using frequency-domain optical coherence tomography. *Arch Ophthalmol*. 2009;127:875–881, doi:10.1001/archophthalmol.2009.145.
16. Wang DL, et al. Central glaucomatous damage of the macula can be overlooked by conventional OCT retinal nerve fiber layer thickness analyses. *Transl Vis Sci Technol*. 2015;4:4, doi:10.1167/tvst.4.6.4.
17. Smith ND, Glen FC, Monter VM, Crabb DP. Using eye tracking to assess reading performance in patients with glaucoma: a within-person study. *Journal of Ophthalmology*. 2014;2014:120528, doi:10.1155/2014/120528.
18. Mathews PM, Rubin GS, McCloskey M, Salek S, Ramulu PY. Severity of vision loss interacts with word-specific features to impact out-loud reading in glaucoma. *Invest Ophthalmol Vis Sci*, 2015;27:IOVS-14-15462, doi:10.1167/iovs.14-15462.
19. Ramulu PY, Swenor BK, Jefferys JL, Friedman DS, Rubin GS. Difficulty with out-loud and silent reading in glaucoma. *Invest Ophthalmol Vis Sci*. 2013;54:666–672, doi:10.1167/iovs.12-10618.
20. Nguyen AM, van Landingham SW, Massof RW, Rubin GS, Ramulu PY. Reading ability and reading engagement in older adults with glaucoma. *Invest Ophthalmol Vis Sci*. 2014;55:5284–5290, doi:10.1167/iovs.14-14138.
21. Glen FC, Crabb DP, Smith ND, Burton R, Garway-Heath DF. Do patients with glaucoma have difficulty recognizing faces? *Invest Ophthalmol Vis Sci*. 2012;53:3629–3637, doi:10.1167/iovs.11-8538.
22. Glen FC, Smith ND, Crabb DP. Saccadic eye movements and face recognition performance in patients with central glaucomatous visual field defects. *Vision Res*. 2013;82:42–51, doi:10.1016/j.visres.2013.02.010.
23. Kwon M, Liu R, Patel BN, Girkin C. Slow reading in glaucoma: is it due to the shrinking visual span in central vision? *Invest Ophthalmol Vis Sci*. 2017;58:5810–5818, doi:10.1167/iovs.17-22560.
24. Chien L, Liu R, Girkin C, Kwon M. Higher contrast requirement for letter recognition and macular RGC+ layer thinning in glaucoma patients and older adults. *Invest Ophthalmol Vis Sci*. 2017;58:6221–6231, doi:10.1167/iovs.17-22621.
25. Nelson P, Aspinall P, O'Brien C. Patients' perception of visual impairment in glaucoma: a pilot study. *Br J Ophthalmol*. 1999;83:546–552.
26. Aspinall PA, et al. Evaluation of quality of life and priorities of patients with glaucoma. *Invest Ophthalmol Vis Sci*. 2008;49:1907–1915, doi:10.1167/iovs.07-0559.
27. Duke-Elder S. In: *System of Ophthalmology Vol. XI*. London: Henry Kimpton; 1969:443.
28. Viswanathan AC, McNaught AI, Poinoosawmy D, et al. Severity and stability of glaucoma: patient perception compared with objective measurement. *Arch Ophthalmol*. 1999;117:450–454.
29. Fujita K, Yasuda N, Oda K, Yuzawa M. [Reading performance in patients with central visual field disturbance due to glaucoma]. *Nippon Ganka Gakkai Zasshi*. 2006;110:914–918.

Downloaded from intl.iovs.org on 08/15/2022

30. McKean-Cowdin R, et al. Impact of visual field loss on health-related quality of life in glaucoma: the Los Angeles Latino Eye Study. *Ophthalmology*. 2008;115:941–948.e941, doi:10.1016/j.ophtha.2007.08.037.
31. Brown JC, Goldstein JE, Chan TL, Massof R, Ramulu P. Low Vision Research Network Study Group. Characterizing functional complaints in patients seeking outpatient low-vision services in the United States. *Ophthalmology*. 2014;121:1655–1662.
32. Ogata NG, Boer ER, Daga FB, Jammal AA, Stringham JM, Medeiros FA. Visual crowding in glaucoma. *Invest Ophthalmol Vis Sci*. 2019;60:538–543.
33. Stringham J, Jammal AA, Mariottoni EB, Estrela T, Urata C, Shigueoka L, Ogata N, Tseng H, Medeiros F. Visual crowding in glaucoma: Structural and functional relationships. *Invest Ophthalmol Vis Sci*. 2020;61:3214–3214.
34. Stievenard A, Rouland J, Peyrin C, Warniez A, Boucart M. Sensitivity to central crowding for faces in patients with glaucoma. *J Glaucoma*. 2021;30:140–147.
35. Kwon M, Liu R. Linkage between retinal ganglion cell density and the nonuniform spatial integration across the visual field. *Proc Natl Acad Sci USA*. 2019;116:3827–3836, doi:10.1073/pnas.1817076116.
36. Kwon M, Patel B, Liu R, Girkin CA. The shrinking visual span may explain glaucomatous reading deficits. *Invest Ophthalmol Vis Sci*. 2016;57:1945–1945.
37. Bouma H. Interaction effects in parafoveal letter recognition. *Nature*. 1970;226:177–178.
38. Levi DM. Crowding—an essential bottleneck for object recognition: a mini-review. *Vision Res*. 2008;48:635–654.
39. Levi DM, Song S, Pelli DG. Amblyopic reading is crowded. *J Vis*. 2007;7:21.21–17, doi:10.1167/7.2.21.
40. Pelli DG, Tillman KA. The uncrowded window of object recognition. *Nat Neurosci*. 2008;11:1129–1135.
41. Pelli DG, et al. Crowding and eccentricity determine reading rate. *J Vis*. 2007;7:20.21–36, doi:10.1167/7.2.20.
42. He Y, Legge GE, Yu DY. Sensory and cognitive influences on the training-related improvement of reading speed in peripheral vision. *J Vis*. 2013;13:14, doi:10.1167/13.7.14.
43. Liu R, Patel BN, Kwon M. Age-related changes in crowding and reading speed. *Sci Rep*. 2017;7:8271–8271, doi:10.1038/s41598-017-08652-0.
44. Kwon M, Bao P, Millin R, Tjan BS. Radial-tangential anisotropy of crowding in the early visual areas. *J Neurophysiol*. 2014;112:2413–2422, doi:10.1152/jn.00476.2014.
45. Pelli DG. Crowding: a cortical constraint on object recognition. *Curr Opin Neurobiol*. 2008;18:445–451, doi:10.1016/j.conb.2008.09.008.
46. Parkes L, Lund J, Angelucci A, Solomon JA, Morgan M. Compulsory averaging of crowded orientation signals in human vision. *Nat Neurosci*. 2001;4:739–744.
47. Balas B, Nakano L, Rosenholtz R. A summary-statistic representation in peripheral vision explains visual crowding. *J Vis*. 2009;9:13.1–18, doi:10.1167/9.12.13.
48. Freeman J, Simoncelli EP. Metamers of the ventral stream. *Nat Neurosci*. 2011;14:1195–1201, doi:10.1038/nn.2889.
49. Greenwood JA, Bex PJ, Dakin SC. Positional averaging explains crowding with letter-like stimuli. *Proc Natl Acad Sci USA*. 2009;106:13130–13135, doi:10.1073/pnas.0901352106.
50. He S, Cavanagh P, Intriligator J. Attentional resolution and the locus of visual awareness. *Nature*. 1996;383:334–337, doi:10.1038/383334a0.
51. Harrison WJ, Bex PJ. A unifying model of orientation crowding in peripheral vision. *Curr Biol*. 2015;25:3213–3219, doi:10.1016/j.cub.2015.10.052.
52. Whitney D, Levi DM. Visual crowding: a fundamental limit on conscious perception and object recognition. *Trends Cogn Sci*. 2011;15:160–168, doi:10.1016/j.tics.2011.02.005.
53. Toet A, Levi DM. The two-dimensional shape of spatial interaction zones in the parafovea. *Vision Res*. 1992;32:1349–1357.
54. Pelli DG, Palomares M, Majaj NJ. Crowding is unlike ordinary masking: distinguishing feature integration from detection. *J Vis*. 2004;4:1136–1169, doi:10:1167/4.12.12.
55. Greenwood JA, Tailor VK, Sloper JJ, Simmers AJ, Bex PJ, Dakin SC. Visual acuity, crowding, and stereo-vision are linked in children with and without amblyopia. *Invest Ophthalmol Vis Sci*. 2012;53:7655–7665, doi:10.1167/iovs.12-10313.
56. Bonneh YS, Sagi D, Polat U. Spatial and temporal crowding in amblyopia. *Vision Res*. 2007;47:1950–1962, doi:10.1016/j.visres.2007.02.015.
57. Dorr M, Kwon M, Lesmes LA, et al. Binocular summation and suppression of contrast sensitivity in strabismus, fusion and amblyopia. *Front Hum Neurosci*. 2019;13:234. doi:10.3389/fnhum.2019.00234.
58. Campbell FW, Green DG. Monocular versus binocular visual acuity. *Nature*. 1965;208:191–192, doi:10.1038/208191a0.
59. Arditi AR, Anderson PA, Movshon JA. Monocular and binocular detection of moving sinusoidal gratings. *Vision Res*. 1981;21:329–336, doi:10.1016/0042-6989(81)90160-7.
60. Legge GE. Binocular contrast summation—II. Quadratic summation. *Vision Res*. 1984;24:385–394, doi:10.1016/0042-6989(84)90064-6.
61. Blake R, Sloane M, Fox R. Further developments in binocular summation. *Percept Psychophys*. 1981;30:266–276, doi:10.3758/bf03214282.
62. Baker DH, Meese TS, Mansouri B, Hess RF. Binocular summation of contrast remains intact in strabismic amblyopia. *Invest Ophthalmol Vis Sci*. 2007;48:5332–5338, doi:10.1167/iovs.07-0194.
63. Hodapp E, Parrish RK, II, Anderson DR. *Clinical decisions in glaucoma*. St Louis: The CV Mosby Co., 1993; 52–61.
64. Brainard DH. The Psychophysics Toolbox. *Spat Vis*. 1997;10:433–436.
65. Pelli DG. The VideoToolbox software for visual psychophysics: transforming numbers into movies. *Spat Vis*. 1997;10:437–442.
66. Wetherill GB, Levitt H. Sequential estimation of points on a psychometric function. *Br J Math Stat Psychol*. 1965;18:1–10, doi:10.1111/j.2044-8317.1965.tb00689.x.
67. R Core Team. *R: A language and environment for statistical computing*. Vienna: R Foundation for Statistical Computing. 2012.
68. Siman-Tov Z, Lev M, Polat U. Binocular summation is affected by crowding and tagging. *Sci Rep*. 2021;11:4843, doi:10.1038/s41598-021-83510-8.
69. Barlow HB, Blakemore C, Pettigrew JD. The neural mechanism of binocular depth discrimination. *J Physiol*. 1967;193:327–342, doi:10.1113/jphysiol.1967.sp008360.
70. Pettigrew JD, Nikara T, Bishop PO. Binocular interaction on single units in cat striate cortex: simultaneous stimulation by single moving slit with receptive fields in correspondence. *Exp Brain Res*. 1968;6:391–410, doi:10.1007/bf00233186.
71. Levi DM, Klein SA. Vernier acuity, crowding and amblyopia. *Vision Res*. 1985;25:979–991.
72. Chung ST, Li RW, Levi DM. Learning to identify near-acuity letters, either with or without flankers, results in improved letter size and spacing limits in adults with amblyopia. *PloS One*. 2012;7:e35829, doi:10.1371/journal.pone.0035829.
73. Song S, Levi DM, Pelli DG. A double dissociation of the acuity and crowding limits to letter identification, and the

Investigative Ophthalmology & Visual Science

Downloaded from intl.iovs.org on 08/15/2022

promise of improved visual screening. *J Vis*. 2014;14:3, doi:10.1167/14.5.3.

74. Shou T, Liu J, Wang W, Zhou Y, Zhao K. Differential dendritic shrinkage of α and β retinal ganglion cells in cats with chronic glaucoma. *Invest Ophthalmol Vis Sci*. 2003;44:3005, doi:10.1167/iovs.02-0620.
75. Levi DM, Klein SA, Hariharan S. Suppressive and facilitatory spatial interactions in foveal vision: foveal crowding is simple contrast masking. *J Vis*. 2002;2:140–166, doi:10.1167/2.2.2.
76. Kooi FL, Toet A, Tripathy SP, Levi DM. The effect of similarity and duration on spatial interaction in peripheral vision. *Spat Vis*. 1994;8:255–279.
77. Chicherov V, Plomp G, Herzog MH. Neural correlates of visual crowding. *Neuroimage*. 2014;93:23–31.
78. Freeman J, Chakravarthi R, Pelli DG. Substitution and pooling in crowding. *Atten Percept Psychophys*. 2012;74:379–396.
79. Strasburger H, Harvey LO, Jr., Rentschler I. Contrast thresholds for identification of numeric characters in direct and eccentric view. *Percept Psychophys*. 1991;49:495–508.
80. Nandy AS, Tjan BS. Saccade-confounded image statistics explain visual crowding. *Nat Neurosci*. 2012;15:463–469, s461–s462, doi:10.1038/nn.3021.
81. Wilkinson F, Wilson HR, Ellemberg D. Lateral interactions in peripherally viewed texture arrays. *J Opt Soc Am A Optics Image Sci Vis*. 1997;14:2057–2068.
82. Redmond T, Garway-Heath DF, Zlatkova MB, Anderson RS. Sensitivity loss in early glaucoma can be mapped to an enlargement of the area of complete spatial summation. *Invest Ophthalmol Vis Sci*. 2010;51:6540–6548, doi:10.1167/iovs.10-5718.
83. Mulholland PJ, Redmond T, Garway-Heath DF, Zlatkova MB, Anderson RS. Spatiotemporal summation of perimetric stimuli in early glaucoma. *Invest Ophthalmol Vis Sci*. 2015;56:6473–6482, doi:10.1167/iovs.15-16921.
84. Pan F, Swanson WH. A cortical pooling model of spatial summation for perimetric stimuli. *J Vis*. 2006;6:1159–1171, doi:10.1167/6.11.2.
85. Fellman RL, Lynn JR, Starita RJ, Swanson WH. *Clinical importance of spatial summation in glaucoma*. Berkeley: Kugler and Gedini; 1989:313–324.
86. Wall M, Lefante J, Conway M. Variability of high-pass resolution perimetry in normals and patients with idiopathic intracranial hypertension. *Invest Ophthalmol Vis Sci*. 1991;32:3091–3095.
87. Chauhan BCH, House PH, McCormick TA, LeBlanc RP. Comparison of conventional and high-pass resolution perimetry in a prospective study of patients with glaucoma and healthy controls. *Arch Ophthalmol*. 1999;117:24–33.
88. King WM, et al. Expansion of visual receptive fields in experimental glaucoma. *Vis Neurosci*. 2006;23:137–142, doi:10.1017/s0952523806231122.
89. Hood DC, Raza AS, de Moraes CGV, Liebmann JM, Ritch R. Glaucomatous damage of the macula. *Prog Retin Eye Res*. 2013;32:1–21.
90. Zhang C, Tatham AJ, Weinreb RN, et al. Relationship between ganglion cell layer thickness and estimated retinal ganglion cell counts in the glaucomatous macula. *Ophthalmology*. 2014;121:2371–2379.
91. Antwi-Boasiako K, Carter-Dawson L, Harwerth R, Gondo M, Patel N. The relationship between macula retinal ganglion cell density and visual function in the nonhuman primate. *Invest Ophthalmol Vis Sci*. 2021;62:5–5.

Investigative Ophthalmology & Visual Science

Downloaded from intl.iovs.org on 08/15/2022